UpWind	Project funded by the European Commission under the 6th (EC) RTD Framework Programme (2002- 2006) within the framework of the specific research and technological development programme “Integrating and strengthening the European Research Area”

Project UpWind

Contract No.:
019945 (SES6)

“Integrated Wind Turbine Design”

Author:	David Schlipf
Affiliation:	Endowed Chair of Wind Energy at Institute of Aircraft Design, Universität Stuttgart
Address:	Allmandring 5B, 70569 Stuttgart, Germany
Tel.:	+49 711 685-68254
Email:	schlipf@ifb.uni-stuttgart.de
Further Authors:	Ervin Bossanyi, Carlo Enrico Carcangiu, Tim Fischer, Timo Maul, Michele Rossetti
Reviewer:	Tim Fischer
Approver:	

Document Information

Document Type	Report
Document Name:	LIDAR assisted collective pitch control
Document Number:	Deliverable D5.1.3
Revision:	A
Rev.Date:	
Classification:	R0: General public
Status:	

Abstract: This document describes how the LIDAR technology can be used to improve collective pitch control.

Contents

STATUS, CONFIDENTIALITY AND ACCESSIBILITY										
Status				Confidentiality				Accessibility	
S0	Approved/Released	●		R0	General public	●		Private web site	
S1	Reviewed			R1	Restricted to project members			Public web site	●
S2	Pending for review			R2	Restricted to European. Commission			Paper copy	
S3	Draft for comments			R3	Restricted to WP members + PL				
S4	Under preparation			R4	Restricted to Task members +WPL+PL				

PL: *Project leader* **WPL:** *Work package leader* **TL:** *Task leader*

1. Introduction

Nacelle based pulsed LIDAR (Light detection and ranging) systems provide preview information of wind disturbances at various distances in front of wind turbines. In previous work [1] it has been shown that this information can be used to improve the speed regulation of wind turbines by a look-ahead update to the collective pitch control, which indicates load reduction of tower and blades. In the scope of the UpWind project a first fatigue and extreme load analysis has been done to concretize the improvement of look-ahead collective pitch control using LIDAR.

In this document the basic idea of the controller is presented in Chapter 2 and its implementation is described in Chapter 3. Chapter 4 shows the results and Chapter 5 concludes the presented work.

2. Predictive feedforward collective pitch control

The primary control goal of the collective pitch feedback controller Σ_{FB} is to maintain the rated generator speed Ω_{rated} in the presence of varying wind v v above the rated wind speed by adjusting the collective pitch angle θ (see Figure 1).

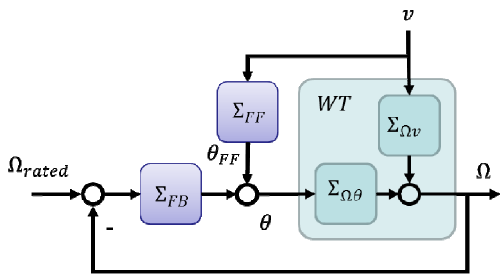

Figure 1: Collective pitch control loop with feedback and feedforward controller.

In theory, known disturbance as the varying wind can be exactly compensated by a feed-forward controller Σ_{FF}, if the influence on the generator speed of the actual wind $\Sigma_{\Omega v}$ $\Sigma_{\Omega v}$ and pitch angle $\Sigma_{\Omega\theta}$ is known and $\Sigma_{\Omega\theta}$ is invertible. Then the update to the feedback output is

$$\Sigma_{FF} = -\Sigma_{\Omega\theta}{}^{-1}\Sigma_{\Omega v} \, ,$$

which compensates the disturbance entirely. Due to its complexity, this perfect compensation cannot be found for an aero-elastic model of a wind turbine and a wind disturbance in form of a stochastic vector field. Therefore in [1] the wind field was reduced to a rotor effective wind speed v_0, and a static compensation was proposed, equivalent to the nonlinear function $\theta_{ss}\left(v_{ss}\right)$ of the static pitch angle θ_{ss} over the static wind speed v_{ss} (see Figure 2).

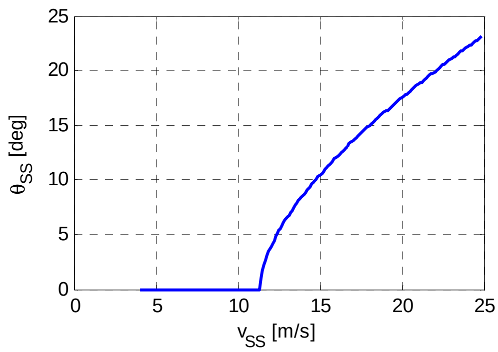

Figure 2: Static pitch angle for static wind speeds.

Due to the higher relative degree of $\Sigma_{\Omega\theta}$ compared to $\Sigma_{\Omega v}$, it is beneficial to use the value of v_0 shifted with τ ahead in time. The feedforward controller is then

$$\theta_{FF}(t) = \theta_{ss}(v_0(t-\tau)).$$

Using this feed-forward law the pitch actuator counteracts to the wind by applying the pitch value corresponding to the actual wind ahead in time. This is beneficial, since the control action has to pass through the pitch actuator dynamics and the predictive time shift is chosen to overcome this transition time.

The advantages of this simple update are that it does not influence the stability of the control loop and it depends only on few parameters.

3. Implementation

For a detailed load analysis for the LIDAR look ahead controller, the UpWind reference turbine is used on a monopile in 20m water depth [2]. Measurements of a LIDAR system were implemented in aero-elastic tool GH Bladed. A reference controller [3], including amongst other things individual pitch control and tower vibration damping, is extended by an update from the processed simulated measurements (see Figure 3).

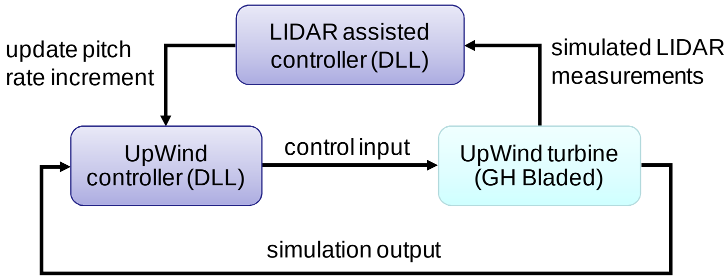

Figure 3: Scope of implementation of the look ahead controller assisted by LIDAR

3.1 Simulation of LIDAR measurements

To realistically reproduce the LIDAR measurements, the generic wind field used for the aero-elastic simulations is evaluated online in GH Bladed according to the characteristics of a real nacelle based LIDAR system. Figure 4 illustrates a mounting example from SWE.

Figure 4: Nacelle mounted SWE LIDAR system [4].

Figure 5 shows the chosen circle scan, which provides twelve measurements every 2s in five distances from 0.5 D to 1.5 D with the rotor diameter D =126m.

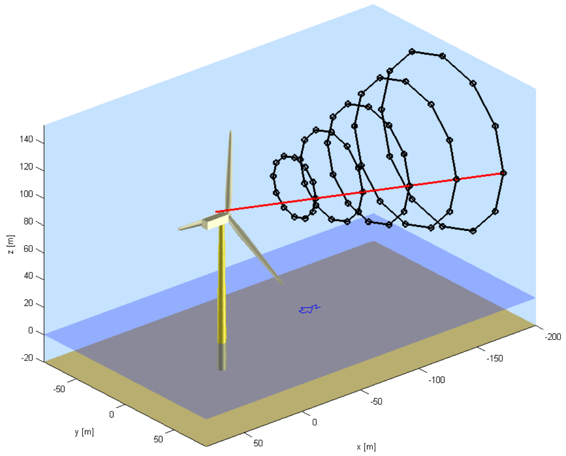

Figure 5: Scope of simulated LIDAR measurements.

For the simulation of the measurement, Taylor's frozen turbulence hypothesis is considered to be valid for all frequencies, assuming the turbulent wind field to be unaffected when approaching the rotor and moving with average wind speed. To simulate for an instant a measurement in 1 D distance during time t of a wind field with mean wind $\bar{u}$ the wind field is analyzed at $t+D/\bar{u}$.

As in reality, only the component of the wind vector in laser beam direction (line-of-sight wind speed) is detected. Volume measurements are considered for each measurement by calculating the line-of-sight wind speeds for a pulse with the pulse length l =60m in various points along the laser beam and applying a weighting function $f(r)$ (see Figure 6)

$$f(r)=\frac{12(|r|-l/2)^2}{l^3} ,$$

with respect to the distance $r \in [-l/2 \quad l/2]$ from the focus point:

$$v_{los}=\int_{-\frac{l}{2}}^{\frac{l}{2}}\left(x_l u(r)+y_l v(r)+z_l w(r)\right) f(r)\, dr ,$$

where $[x_l \quad y_l \quad z_l]^T$ is the laser beam direction and u, v, w are the longitudinal, lateral, and upward velocity components respectively.

The advantage of a pulsed system is that accurate measurements can be done close to the rotor simultaneously with measurements farther away to detect gusts on time.

The line-of-sight wind speeds are passed to an external dynamic link library (DLL) which processes the simulated LIDAR measurements and provides the pitch rate increment to the controller DLL.

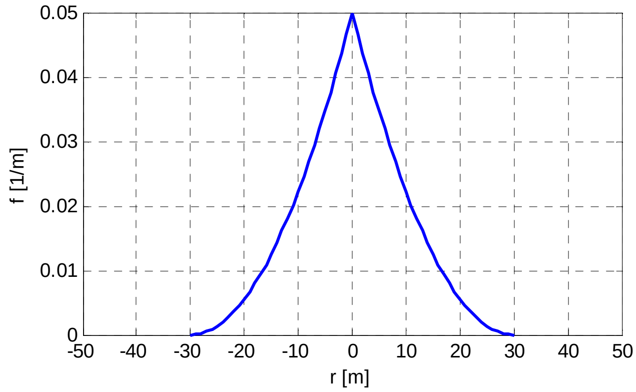

Figure 6: Weighting function for the simulated pulsed LIDAR [5].

3.2 Processing of LIDAR measurements

In the external DLL the incoming wind component for each focus point is reconstructed using the assumption of perfect alignment with the wind ($v = w = 0$):

$$u = \frac{v_{los}}{x_l},$$

and then averaged for each circle over the last trajectory. The five time series measured in the five distances simultaneously by the LIDAR are time shifted according to Taylor's frozen turbulence hypothesis (distance divided by mean wind speed) and combined to one wind speed v_0. The moving average over all points of a trajectory is necessary to obtain a rotor effective wind speed independent of vertical and horizontal shears. Due to the combination of the different time series the information gathered in different radial positions is used.

Only turbulences with a wave number below $\hat{k}$=0.06rad/m have been detected by a nacelle based LIDAR system up to now [6]. Contrary to the simulation of the LIDAR measurement, the processing of the data has to be low pass filtered depending of the mean wind speed $\bar{u}$ with the corresponding cut off frequency

$$f_{cutoff} = \frac{\hat{k}\bar{u}}{2\pi}$$

to account for uncertainties of Taylor's frozen turbulence hypothesis and to avoid incorrect pitch action. Here a second order Butterworth filter is used.

3.3 Determination of the pitch rate increment

In contrast to Figure 1, an update $\dot{\theta}_{FF}$ to the pitch rate increment is chosen for simplicity in the implementation. Therefore,Σ_{FFs} is modified to

$$\dot{\theta}_{FF}(t) = \dot{v}_0(t-\tau)\frac{d\theta_{ss}}{dv_{ss}}\left(v_0(t-\tau)\right).$$

The advantage of using $d\theta_{ss}/dv_{ss}$ instead of using a derivative of $\theta_{ss}(v_{ss})$ is, that the transition from below rated to rated wind speed can easily be smoothed. Figure 7 shows the used feedforward law limited to 5°s/m. With this limit, still higher loads have been observed in the transition region between partial and rated load through strong changes in the thrust.

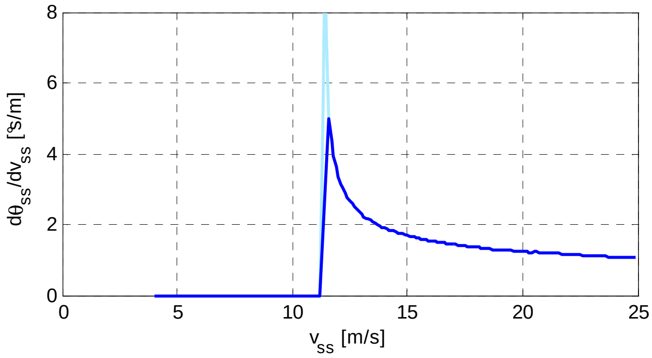

Figure 7: Theoretical (light blue) and limited (dark blue) feedforward law.

As an example **Figure 8** shows the perfect transition (black) in terms of load reduction, which would be to change slowly from the peak value at rated wind speed (ca. at *t*=306s) to the corresponding value of above rated wind speed (ca. at *t* > 313s). The UpWind controller combined with the feedforward controller (red) shows a worse behaviour than the baseline UpWind controller (dark blue). In a first improvement with a limitation of the pitch rate increment to +/- 0.3°/s for 11.2m/s< v_0 <12.5m/s, the loads are reduced significantly (see Table 1).

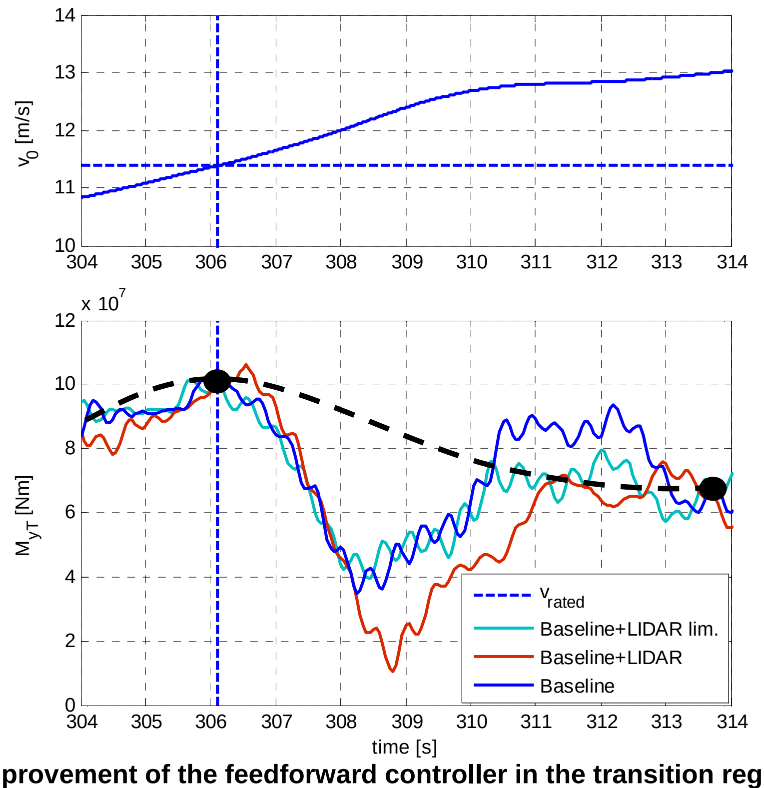

Figure 8: Improvement of the feedforward controller in the transition region through a limitation of the pitch rate increment.

Controller	DEL [m=4], [MNm] M_{yT}
Baseline	94.1
Baseline+LIDAR	98.9
Baseline+LIDAR lim.	79.6

Table 1: Damage Equivalent Loads (N=2E06) for the 10min simulation with 12m/s.

3.4 Controller parameters

The parameters for the collective pitch feedback controller and the prediction time are first determined by spectra estimation [7] and then iteratively improved by simulations.

The feedback controller for the collective pitch is modified, if the feedforward is used:

- Proportional Gain 0.00675 Nms/rad (half of old value)
- Integral Gain 0.0011325 Nms/rad (quarter of old value)

All other parameters of the UpWind controller are unchanged.

Considering Chapter 2, the prediction time depends on the pitch actuator dynamics only. But with the optimization over estimated spectra a dependency on the mean wind speed can be observed. Through simulations, slightly better results have been made with a higher but still mean wind speed dependent prediction time. This investigation has been made for better understanding because in general the feedforward is quite robust and also for constant prediction time (1s) the results do not change significantly.

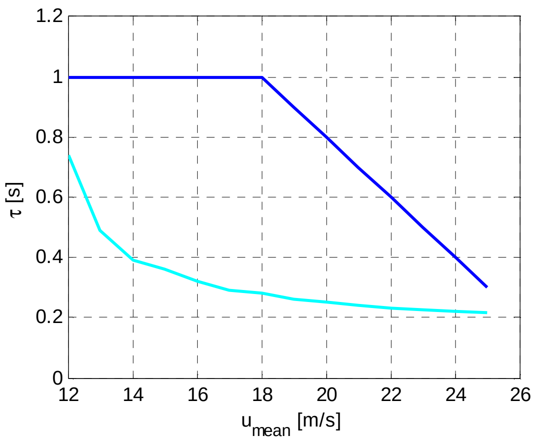

Figure 9: The prediction time from the spectra estimation τ_{Spec} (light blue) and obtained through optimisation via simulations τ_{Sim} (dark blue).

4. Results

A load envelope according to current standards [8] is done and, based on that, the controller potential is illustrated in terms of turbine fatigue and extreme loads.

4.1 Results for fatigue loads

In the first step various simulations with a Rayleigh distribution (A=12m/s) and wind turbulence class A according to [8] were analysed, to estimate the load reduction potential of the proposed controller for fatigue loads. Bins of 2m/s from 4 to 24 m/s had been chosen, each simulated with 3 different seeds.

The effect of using LIDAR assisted control can be observed clearly in the frequency domain (see Figure 10): The controller with the feedforward can significantly reduce the influence of the wind disturbance to rotor speed and to the tower base fore-aft bending moment below the 1P-frequency. Also the pitch rate is reduced in this region.

The standard deviation of rotor speed and the damage equivalent loads (DEL) over the different wind speeds can be seen in Figure 11. Both feedforward controllers show a good improvement compared to the UpWind controller used alone, but with τ_{Sim} slightly better results can be achieved compared to τ_{Spec} (Table 2). This indicates a robustness of the feedforward controller regarding the prediction time.

Controller	DEL (m=4), M_{yT} [MNm]	Reduction
Baseline	107.6	0%
Baseline+LIDAR τ_{Sim}	85.7	-20.4%
Baseline+LIDAR τ_{Spec}	86.9	-19.2%

Table 2: Lifetime weighted Damage Equivalent Loads (20 years, N=2E06) of tower base fore-aft bending moment for different controllers and prediction time τ_{Sim} .

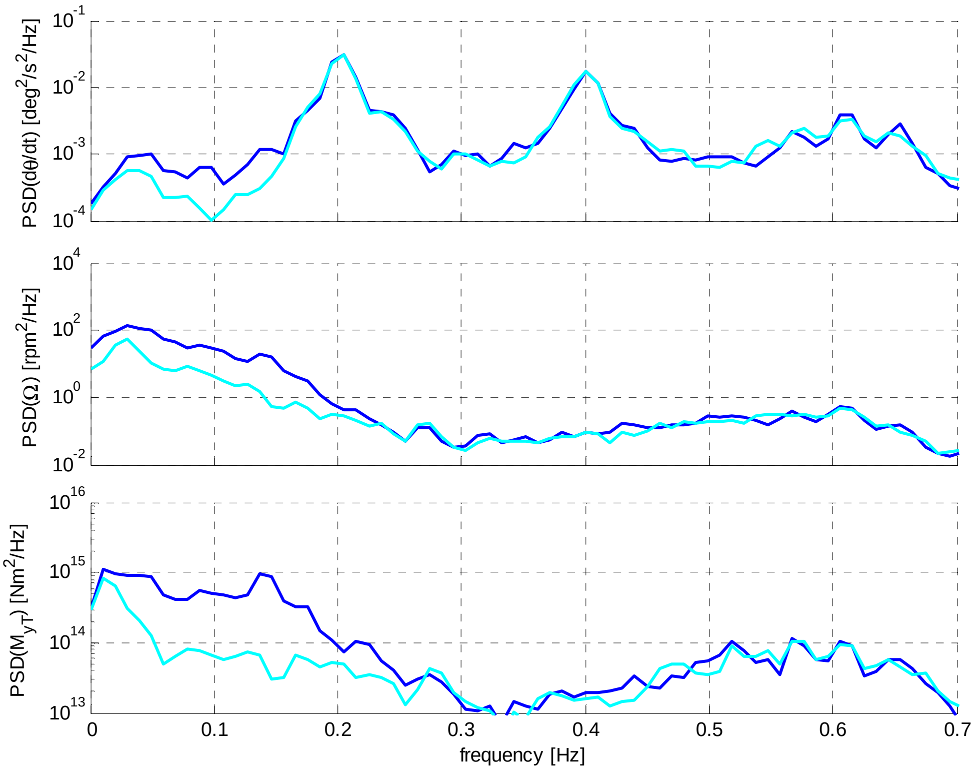

Figure 10: Power spectral density of pitch rate, rotor speed and tower base fore-aft bending moment for a simulation with 16 m/s, UpWind controller only (dark blue) and with feedforward and prediction time τ_{Sim} (light blue).

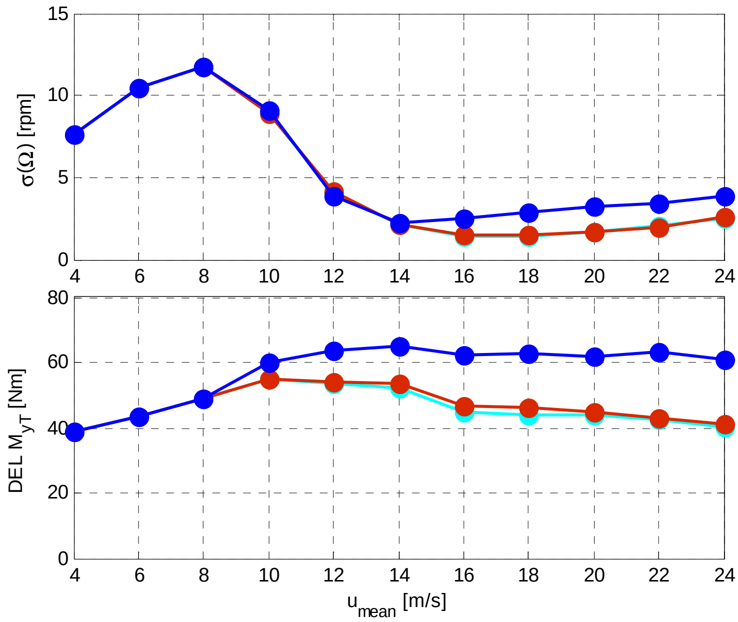

Figure 11: Average of standard deviation of the generator speed and 20 years lifetime weighted DEL of the tower base fore-aft bending moment for UpWind controller only (dark blue) and with feedforward (τ_{Sim} light blue, τ_{Spec} red).

In the next step several simulations have been run using Rayleigh distributions with A=10 and 12m/s, and wind turbulence class A and B to estimate influence of wind distribution and turbulence to the benefit of LIDAR assisted control, see Table 3.

The best reduction is achieved for high wind speeds. The wind turbine class has more effect on blade out-of-plane root bending moment. No significant effects on other loads can be observed.

WT Class	Rayleigh A [m/s]	Reduction DEL (m=4) M_{yT}	Reduction DEL (m=10) M_{yB}
A	12	-20.4 %	-11.4%
A	10	-15.8 %	-9.2 %
B	12	-19.5 %	-8.3 %
B	10	-15.7 %	-6.1 %

Table 3: Reduction of lifetime weighted Damage Equivalent Loads (20 years, N=2E06) of tower base fore-aft and out-of-plane blade root bending moment for the feedforward controller for different wind distributions and wind turbine classes.

4.2 Results for extreme loads

Figure 12 compares the pitch angle, rotor speed, and tower base bending moment for an “Extreme Operating Gust” according to current guidelines [8] for the UpWind controller and the LIDAR assisted controller. Additionally, the detection of the gust by the LIDAR system is plotted, showing the effect of spatial and temporal filtering.

The maximum absolute deviation of rotor speed and tower base fore-aft moment can be reduced from 20% to 2% and 302% to 60%, respectively (see Figure 12). Of course this gust case has to be recognised as rather artificial.

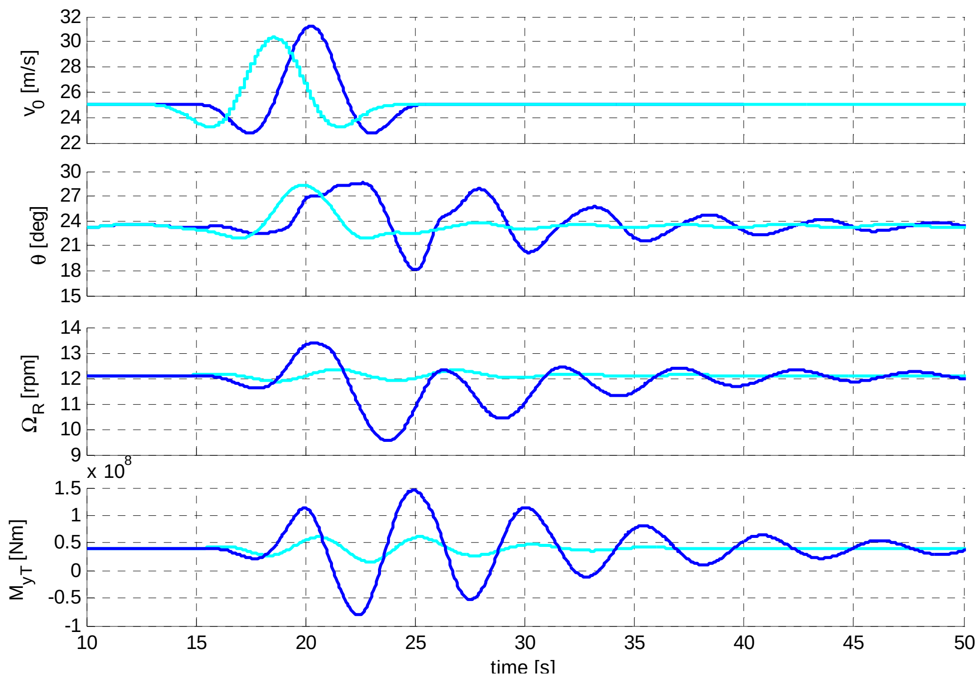

Figure 12: top: Wind gust (dark blue) and LIDAR measurement (light blue); rest: collective pitch angle, rotor speed and tower base fore-aft bending moment for UpWind controller only (dark blue) and with feedforward (light blue).

5. Conclusions

In this work a LIDAR simulator has been successfully coupled to GH Bladed. With this tool it was possible to estimate in a realistic way the benefit of LIDAR assisted collective pitch control by comparing it to the sophisticated UpWind controller.

First results show that it is possible to reduce fatigue loads on tower and blades up to 20% and 10% respectively. This reduction is due to compensation of the dynamic below the 1P frequency, where most of the rotor speed variation and tower base fore-aft bending moment variation occur. For the used turbine the 1P frequency is near the cut-off frequency which has to be used for filtering the LIDAR data due to uncertainties of Taylor’s frozen turbulence hypothesis. Therefore the validated frequency domain for Taylor’s hypothesis is sufficient for predictive collective pitch control. Further improvement can be made by better determination of the rotor effective wind speed by LIDAR systems with smaller probe volume and better scanning devices.

Even better results could be observed for extreme loads. For the standard (albeit artificial) extreme operating gust a reduction of 80% for the deviation of the tower base fore-aft bending moment from the static value could be achieved (60% reduction in peak value), but will be investigated in more detail in further studies.

6. References

[1] Schlipf, D. and Kühn, M.: *Prospects of a Collective Pitch Control by Means of Predictive Disturbance Compensation Assisted by Wind Speed Measurements*, Proc. DEWEK 2008, Bremen, Germany, November 2008.

[2] Jonkman, J., Buttereld, S., Musial, W., and Scott, G.: *Definition of a 5-MW reference wind turbine for offshore system development*, National Renewable Energy Laboratory (NREL), Boulder, 2009.

[3] Bossanyi, E.: *Controller for 5MW reference turbine*, GH report 11593/BR/04, Bristol, 2009.

[4] Rettenmeier, A., Bischoff, O., Hofsäß, M.,Schlipf, D., Trujillo, J. J., and Kühn, M.: *Wind field analyses using a nacelle-based LIDAR system*, Proc. EWEC, Warsaw, Poland, March 2010.

[5] Lindelöw, P.: *Fiber Based Coherent Lidars for Remote Wind Sensing*, Ph.D. thesis, Danish Technical University, Copenhagen, Denmark, 2008.

[6] Schlipf, D., Trabucchi, D., Bischoff, O., Hofsäß, M., Mann, J., Mikkelsen, T., Rettenmeier, A., Trujillo, J. J., and Kühn, M.: *Testing of Frozen Turbulence Hypothesis for Wind Turbine Applications with a Scanning LIDAR System*, Proc. ISARS, Paris, France, June 2010.

[7] Schlipf, D., Fischer, T., Carcangiu, C.E., Rossetti, M., and Bossanyi, E.: *Load Analysis of Look-Ahead Collective Pitch Control Using LIDAR*, Proc. DEWEK, Bremen, Germany, November 2010.

[8] IEC 61400-1 Ed. 3, Wind Turbines - Part 1: Design requirements, 2005.